Acta Crystallographica Section D
Biological Crystallography
ISSN 0907-4449

The structure of human MRP8, a member of the S100 calcium-binding protein family, by MAD phasing at 1.9 Å resolution

Kohtaro Ishikawa,[a] Atsushi Nakagawa,[a]† Isao Tanaka,[a]* Masaki Suzuki[b] and Jun Nishihira[b]

[a]Division of Biological Sciences, Graduate School of Science, Hokkaido University, Sapporo 060-0810, Japan, and [b]Central Research Institute, School of Medicine, Hokkaido University, Sapporo 060-0815, Japan

† Present address: Institute for Protein Research, Osaka University, 3–2 Yamada-oka, Suita 565–0871, Japan.

Correspondence e-mail: tanaka@castor.sci.hokudai.ac.jp

Received 29 October 1999
Accepted 18 February 2000

PDB Reference: MRP8, 1mr8.

The structure of human MRP8 in the calcium-bound form was determined at 1.9 Å resolution by X-ray crystallography. The structure was initially solved by MAD phasing of an ytterbium-substituted crystal and was refined against data obtained from a Ca^{2+}-bound crystal. The dimeric form of MRP8 was stabilized by hydrophobic interactions between mutually wrapped helices. There were two EF-hand motifs per monomer and each EF-hand bound one Ca^{2+} with a different affinity [the affinity of the C-terminal EF-hand (EF-2) for Ca^{2+} was stronger than that of the N-terminal EF-hand (EF-1)]. Furthermore, replacement with Yb^{3+} occurred in the C-terminal EF-hand only, suggesting a more flexible nature for EF-2 than for EF-1. This, combined with previous observations that the helix in EF-2 (helix III) undergoes a large conformational change upon calcium binding, suggests that the C-terminal EF-hand (EF-2) plays a role as a trigger for Ca^{2+}-induced conformational change.

1. Introduction

In the event of acute or chronic inflammation, infiltrate macrophages express two specific proteins, MRP8 and MRP14 (Odink *et al.*, 1987). These proteins were originally isolated from human peripheral blood mononuclear cell cultures as part of a complex using a monoclonal antibody directed against human macrophage migration inhibitory factor (MIF) and were thus named MIF-related proteins (MRP; Burmeister *et al.*, 1986). Subsequent study showed that these proteins are specifically expressed in human cells of myeloid origin and that their expression is regulated during monocyte–macrophage and granulocyte differentiation (Lagasse & Clerc, 1988). They are expressed in specific stages in acute inflammatory states and also in chronic inflammatory states such as rheumatoid arthritis or sarcoidosis (Odink *et al.*, 1987; Zwadlo *et al.*, 1988; Delabie *et al.*, 1990).

A computer-assisted survey of these proteins using a protein database revealed that they have Ca^{2+}-binding motifs and belong to the S100 family of proteins (Lagasse & Clerc, 1988). The S100 protein family is the largest subfamily of EF-hand proteins (Kligman & Hilt, 1988; Persechini *et al.*, 1989; Schäfer & Heizmann, 1996). Members of this family are all abundant low molecular-weight (10–12 kDa) acidic proteins that are expressed in a cell-specific manner. Most of them exist as homodimers or heterodimers under physiological conditions. The purported functions of S100 proteins include cellular growth and differentiation, cell-cycle regulation, cytoskeletal protein and membrane interaction and Ca^{2+} transport. They are composed of two distinct EF-hand motifs

Table 1
Crystallographic data.

Values in parentheses are for the highest resolution shell {2.00–1.90 Å (native), 2.42–2.30 Å [Yb, Xe (0.7 MPa)] and 2.11–2.00 Å [Xe (2.0 MPa)]}.

		Yb			Xe	
Data	Native	Peak	Edge	Remote	0.7 MPa	2.0 MPa
Wavelength (Å)	1.0000	1.38525	1.38580	1.10000	1.0000	1.0000
Resolution (Å)	40.0–1.9	40.0–2.3	40.0–2.3	40.0–2.3	120.0–2.3	120.0–2.0
Observed reflections	97834 (10549)	63724 (7450)	63720 (7443)	69573 (9355)	44809	66392
Unique reflections	16285 (2129)	8445 (987)	8440 (986)	9327 (1240)	9517	8816
Completeness (%)	96.3 (88.5)	88.3 (73.0)	88.3 (73.0)	97.2 (89.7)	98.3 (93.1)	96.3 (89.3)
Multiplicity	6.0 (5.0)	7.5 (7.5)	7.5 (7.5)	7.5 (7.5)	4.7 (4.0)	4.8 (4.8)
$I/\sigma(I)$	10.1 (2.1)	9.2 (3.2)	9.8 (3.0)	8.3 (2.7)	6.3 (2.1)	9.9 (2.8)
$R_{\rm merge}$†	0.062 (0.334)	0.069 (0.226)	0.068 (0.243)	0.083 (0.257)	0.105 (0.359)	0.062 (0.272)
$R_{\rm anom}$‡	—	0.097 (0.155)	0.085 (0.153)	0.085 (0.137)	—	—
R_{λ}§	—	0.082	0.113	—	—	—
$R_{\rm iso}$¶	—	—	—	—	0.103	0.094

† $R_{\rm merge} = \sum\sum_j |\langle I(h)\rangle - I(h)_j| / \sum\sum_j \langle I(h)\rangle$, where $\langle I(h)\rangle$ is the mean intensity of symmetry-equivalent reflections. Friedel pairs were merged as individual data. ‡ $R_{\rm anom} = \sum\sum|\langle I(+h)\rangle - \langle I(-h)\rangle| / \sum[\langle I(+h)\rangle + \langle I(-h)\rangle]$. § $R_{\lambda} = \sum\sum_j ||F_{\lambda j}| - |F_{\lambda 0}|| / \sum\sum_j |F_{\lambda 0}|$, where $F_{\lambda j}$ is the structure factor of the data collected at λ_j and $F_{\lambda 0}$ is the structure factor of the data collected at remote wavelength (1.10000 Å). ¶ $R_{\rm iso} = \sum\sum_j ||F_{PH}| - |F_P|| / \sum\sum_j |F_P|$, where F_P and F_{PH} are the structure factors of the native and heavy-atom data, respectively.

flanked by hydrophobic regions at either terminus, which are separated by a central hinge region. Some 17 different proteins have been assigned to the S100 protein family (Schäfer & Heizmann, 1996).

It was demonstrated by biochemical analysis that MRP8 and MRP14 could form homodimers and heterodimers (Teigelkamp *et al.*, 1991). Several studies of these proteins showed that most of the phenotypic functions may be exerted by a complex of the two molecules. Accordingly, a variety of complex conformations may elicit different phenotypic functions *in vivo*. To date, no study of the structure–function relationship by means of three-dimensional protein structural analysis has been performed. Here, we reveal the three-dimensional structure of MRP8 by X-ray crystallography in order to examine the structure–function relationship in association with Ca^{2+}. The molecule consists of 93 amino-acid residues and has a molecular weight of 10 835 Da. It exists as a dimer in the crystal. The analysis showed that each MRP8 monomer consists of two helix–loop–helix (EF-hand) motifs and that the two monomers in the asymmetric unit wrap tightly around each other in a helical packing. The N-terminal and C-terminal EF-hands show a clear difference with respect to the replacement of the bound calcium by the lanthanide ion.

2. Materials and methods

2.1. Purification and crystallization

Recombinant human MRP8 was overexpressed in *Escherichia coli* [strain BL21(DE3)LysS] containing a pET-3a expression vector subcloned with the MRP8 cDNA. The protein was purified by anion-exchange chromatography using DE-52 (Whatman) and by gel-column chromatography using Sephadex G-100 (Pharmacia).

Crystallization experiments were carried out using the hanging-drop vapour-diffusion method (McPherson, 1976) by mixing 3 µl of protein solution (10 mg ml^{-1} in H_2O) with 3 µl of reservoir solution. The best crystals were grown from a solution containing 15%(*w*/*v*) PEG 6000, 7%(*v*/*v*) MPD, 0.1 *M* MES pH 6.0, 20 m*M* $CaCl_2$ at 291 K. The maximum dimensions of the crystals were 0.2 × 0.2 × 0.2 mm. Crystallization of the Yb-substituted crystal was performed in the same way, using a protein solution in which $CaCl_2$ was substituted by $Yb(NO_3)_3$. The best crystals were grown from a solution

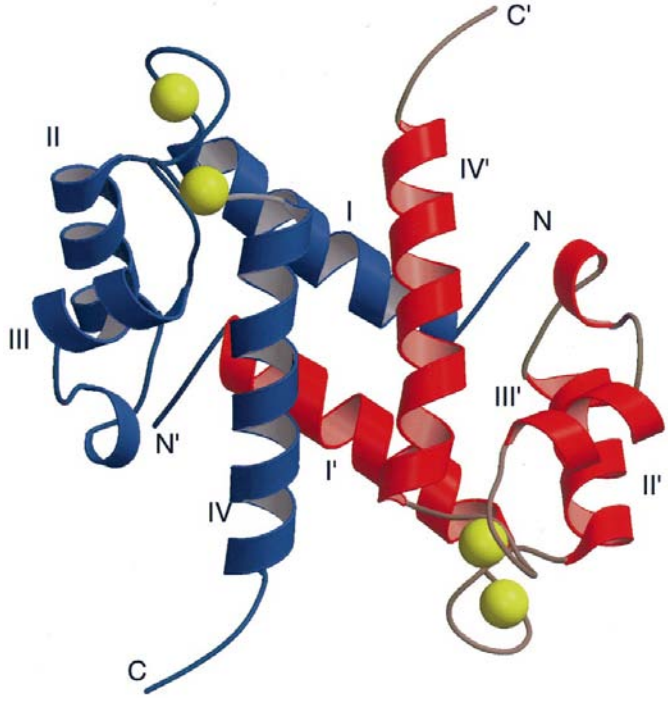

Figure 1
A ribbon representation of the human MRP8 dimer, viewing perpendicular to the twofold non-crystallographic axis. Two monomers are drawn in different colours (blue and red) and the four Ca atoms are shown in yellow. The figure was drawn using the programs *MOLSCRIPT* (Kraulis, 1991) and *Raster3D* (Merrit & Murphy, 1994).

containing 18%(*w*/*v*) PEG 8000, 0.3 *M* sodium acetate, 0.1 *M* MES pH 6.2, 20 m*M* $Yb(NO_3)_3$ at 291 K; the maximum dimensions of the crystals were 0.15 × 0.1 × 0.1 mm. The native (calcium-bound) MRP8 crystal belongs to the trigonal space group $P3_121$, with unit-cell dimensions $a = b = 52.50$ (3), $c = 128.6$ (2) Å, whereas the unit-cell dimensions of the Yb-substituted crystal are $a = b = 51.50$ (2), $c = 127.4$ (2) Å. The crystals contain one dimer per asymmetric unit, with corresponding V_M values of 2.36 Å^3 Da^{-1} (native crystal) and 2.25 Å^3 Da^{-1} (Yb-substituted crystal).

2.2. Data collection

Data-collection statistics are given in Table 1. Native data were collected at a wavelength of 1.0000 Å at room temperature on beamline BL-6B of the Photon Factory, Tsukuba, Japan. MAD data sets (Hendrickson, 1991) were collected at three different wavelengths (1.38525, 1.38580 and 1.10000 Å) from a single Yb-substituted crystal at 100 K on beamline BL-18B. 0.7 MPa Xe crystal data were collected at a wavelength of 1.0000 Å at room temperature on beamline BL-6B and 2.0 MPa Xe crystal data were collected at a wavelength of 1.0000 Å at room temperature on beamline BL-18B. Intensity data were obtained using a Weissenberg camera (Sakabe *et al.*, 1995) and imaging plates as a detector (Miyahara *et al.*, 1986). The data were processed with the *HKL* suite (Otwinowski, 1993) and the *CCP*4 package (Collaborative Computational Project, Number 4, 1994).

2.3. Phase calculation

Two Yb atoms were located from the Bijvoet anomalous difference Patterson map and the isomorphous Patterson map. The program *SHARP* (de la Fortelle & Bricogne, 1997) was used for the refinement of heavy-atom parameters and MAD phase calculation. The initial electron-density map was obtained after phase improvement using the program *SOLOMON* (Abrahams & Leslie, 1996) implemented in *SHARP*. The phasing statistics are given in Table 2. Although we collected Xe-derivative data for the structure analysis as described in §2.5, the map obtained from Yb MAD was sufficiently clear and no phase combination was applied.

2.4. Model building and refinement

The atomic model was built using the graphics program *O* (Jones *et al.*, 1991). Of the 93 residues of each monomer of MRP8, 90 of each were built into the initial electron-density map. Three carboxyl-terminal residues of each monomer were completely disordered and could not be identified in the electron-density map. The model was submitted to rigid-body refinement using the program *X-PLOR* (Brünger, 1993) with native data in the resolution range 10.0–3.0 Å. Simulated-annealing refinement (Brünger *et al.*, 1987) using slow-cooling protocols (Brünger *et al.*, 1990; 8.0–2.0 Å), positional refinement and temperature-factor refinement (8.0–1.9 Å) were performed using the program *X-PLOR*. No NCS constraints were applied for the refinement because of the obvious difference in the conformation of the C-terminal α-helical region of the two monomers in the asymmetric unit. *ARP* (Lamzin & Wilson, 1993) was used to find water molecules in the refinement cycle. At the final stage of *X-PLOR* refinement, the low-resolution limit of the diffraction data was increased from 10 to 20 Å by applying the bulk-solvent correction (Jiang & Brünger, 1994).

The final model has an *R* factor of 19.3% for 90% of the data in the resolution range 20–1.9 Å, including 180 residues (1–90 of each monomer), four Ca atoms (two Ca atoms for each monomer) and 104 water molecules. The free *R* factor (Brünger, 1992) for the remaining 10% of the data within this resolution range is 23.5%. The

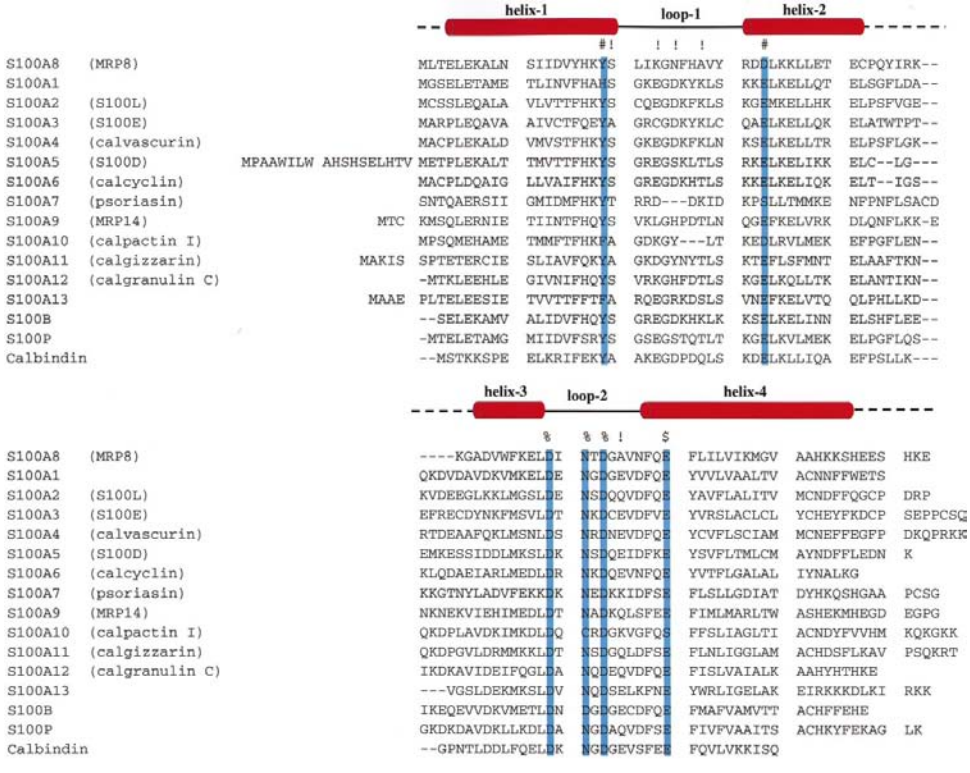

Figure 2
Amino-acid sequence alignment of the S100 proteins. Secondary-structure elements as determined by the present work are also given. Residues which coordinate calcium ions are indicated as follows: !, backbone carbonyl group; #, water-mediated; %, monodentate side chain of Asp or Asn; $, bidentate side chain of Glu. The residues highlighted in blue represent well conserved residues the side chains of which coordinate calcium ions. All sequences were obtained from the SWISS-PROT protein sequence database.

Table 2
Phasing statistics.

	Yb MAD						Xe SIRAS			
Phasing	Peak		Edge		Remote		Xe (0.7 MPa)		Xe (2.0 MPa)	
Data	Isom.	Anom.	Isom.	Anom.	Isom.	Anom.	Isom.	Anom.	Isom.	Anom.
$R_{\rm Cullis}$†										
Centric	0.243	—	0.224	—	—	—	0.679	—	0.585	—
Acentric	0.232	0.231	0.188	0.413	—	0.509	0.661	0.889	0.584	0.964
$R_{\rm Kraut}$‡										
Centric	0.130	0.253	0.158	0.261	0.192	0.308	0.324	0.275	0.347	0.343
Acentric	0.024	0.046	0.028	0.047	0.035	0.056	0.075	0.064	0.062	0.061
Phasing power§										
Centric	10.94	—	7.745	—	—	—	1.831	—	1.820	—
Acentric	19.53	13.82	15.78	8.164	—	6.202	2.270	0.483	1.932	0.436
Figure of merit	Centric: 0.726		Acentric: 0.881				Centric: 0.402		Acentric: 0.285	
After *SOLOMON*¶	0.997						0.920			

† $R_{\rm Cullis} = \sum_j |E|/\sum_j \big||F_\lambda| - |F_{\lambda 0}|\big|$, where E is the lack of closure. ‡ $R_{\rm Kraut} = \langle E\rangle/\langle|F_\lambda|\rangle$, where E is the phase-integrated lack of closure. § Phasing power = $\langle|F_H({\rm calc})|/|E|\rangle$, where F_H(calc) is the calculated anomalous difference and E is the lack of closure. ¶ Figure of merit after density modification by *SOLOMON* (Abrahams & Leslie, 1996).

r.m.s. deviations from standard values of bond lengths and angles are 0.005 Å and 0.966°, respectively. The r.m.s. deviations on superposition of the two monomers are 0.49 Å (Ca atoms of residues 2–70) and 1.32 Å (Ca atoms of residues 1–90). Analysis of the protein geometry was performed using the program *PROCHECK* (Laskowski *et al.*, 1993). All 90 residues were located in the most favoured regions (92.2%) or additional allowed regions (7.8%) of the Ramachandran plot.

2.5. Xenon-binding data

MRP8–xenon complexes were obtained by exposing the native crystals to xenon pressures of 0.7 and 2.0 MPa using a device similar to the one developed by Stowell *et al.* (1996). Derivative data were collected at a wavelength of 1.00 Å at room temperature on beamlines BL-6B and BL-18B (Sakabe *et al.*, 1995). The data were processed using the *HKL* suite (Otwinowski, 1993) and the *CCP*4 package (Collaborative Computational Project, Number 4, 1994). The first two Xe atoms were located in both isomorphous and anomalous difference Patterson maps. The third Xe atom was found during the Xe-atom parameter refinement and phasing using single isomorphous replacement with the anomalous difference effect of a xenon derivative in *SHARP* (de la Fortelle & Bricogne, 1997).

3. Results and discussion

3.1. Structure description

A view of the overall structure of the MRP8 dimer is shown in Fig. 1. Each MRP8 monomer in a calcium-bound state consists of two helix–loop–helix (EF-hand) motifs that are joined by a nine-residue linker (Cys42–Gly50) characteristic of the EF-hand protein. The N-terminal EF-hand (EF-1) consists of helix I (Glu4–Ser20), the calcium-binding loop (Leu21–Tyr30; loop 1) and helix II (Arg31–Glu41). Following the helix II, a proline residue (Pro43) leads to a break in the regular helical pattern and the smaller one-turn helix (Gln44–Arg47) begins in a somewhat different direction. After passing through the helix, the C-terminal EF-hand (EF-2) begins with helix III (Ala51–Leu58), followed by the calcium-binding loop (Asp59–Asn67; loop 2) and finally helix IV (Phe68–Ser86). The packing between helix I and helix IV is stabilized by the interactions of aromatic side chains (Tyr16, Phe68 and Phe71), which make a hydrophobic core as in holo calcyclin (Sastry *et al.*, 1998). As these aromatic residues are conserved in other S100 proteins (Fig. 2), they may contribute as a structure determinant for the overall common fold of the S100 family of proteins.

The MRP8 dimer is formed by non-covalent interactions between the large hydrophobic patches of the two monomers that are related by a non-crystallographic twofold symmetry. The two crystallographically independent MRP8 monomers have an almost identical fold, with slight differences in loop 1 and helix IV. The root-mean-square (r.m.s.) deviations on superposition of the two monomers are 0.49 Å (Ca atoms of residues 2–70) and 1.32 Å (Ca atoms of residues 1–90); the r.m.s. deviations are 0.26 Å for helix I, 0.42 Å for loop 1, 0.21 Å for helix II–III, 0.20 Å for loop 2 and 0.51 Å for helix IV, respectively. The dimer's packing is stabilized by hydrophobic side chains in an antiparallel fashion about helix I–I′ and IV–IV′. Both helical packings are highly symmetric owing to the antiparallel arrangement of the helices.

3.2. Calcium binding at EF-hands

The C-terminal EF-hand (EF-2) of the S100 family of proteins is usually referred to as canonical; its calcium-binding loop is composed of 12 amino-acid residues. The calcium ligands are mostly carboxylate groups of well conserved acidic residues. On the other hand, the N-terminal EF-hand (EF-1) is usually composed of 14 amino-acid residues. The calcium ligands are mostly main-chain carbonyl O atoms and the residues are relatively divergent. The EF-1 usually has lower affinity than EF-2 for Ca^{2+} (Schäfer & Heizmann, 1996).

Table 3
Comparison of the interhelical angles (°) in S100 proteins.

Interhelical angles were calculated using the program *HELIXANG* from the *CCP*4 program package (Collaborative Computational Project, Number 4, 1994). Helices were defined as residues 4–20, 30–42, 51–58, 68–86 in holo MRP8, 2–17, 30–39, 52–58, 70–88 in holo S100B, 1–17, 29–39, 50–62, 70–83 in apo S100B, 3–15, 25–35, 46–54, 63–73 in holo calbindin and 3–14, 25–35, 47–53, 63–73 in apo calbindin. Shown values are each the average of the value of several structures. The coordinates for holo S100B (1uwo), apo S100B (1cfp), holo calbindin (3icb) and apo calbindin (1clb) were obtained from the Protein Data Bank.

Helices	Holo MRP8	Holo S100B	Apo S100B	Holo calbandin	Apo calbandin
I–II	135 (±2)	143 (±9)	128 (±9)	134	123 (±4)
II–III	110 (±0)	133 (±13)	141 (±8)	111	106 (±12)
III–IV	111 (±1)	138 (±10)	165 (±16)	128	115 (±21)
IV–I	129 (±0)	109 (±5)	114 (±6)	121	119 (±6)

The Ca^{2+} coordination by the N-terminal and C-terminal EF-hands of MRP8 are shown in Figs. 3(*a*) and 3(*b*), respectively. In the case of EF-1 of MRP8, 14 residues (Ser20–Asp33) form a (non-canonical) EF-hand calcium-binding loop where four main-chain carbonyl groups, Ser20, Lys23, Asn25 and Ala28, make four ligands to the central Ca^{2+}. In ordinal EF-1, the fifth ligand is a side-chain O atom of the well conserved glutamic acid (Fig. 2). However, in MRP8, the corresponding residue was replaced by aspartic acid (Asp33), which has a shorter side chain. Because of this change, the O atom of Asp33 is not directly ligated to the Ca^{2+}, but a water molecule bridges the O atom of Asp33 and the Ca^{2+}. There is no sixth ligand for MRP8. This position is usually occupied by a water molecule (Szebenyi & Moffat, 1986; Matsumura *et al.*, 1998).

As in C-terminal EF-2, MRP8 contains all the residues needed for calcium binding (Asp59–Glu70). Seven oxygen ligands (the main-chain carbonyl group of Ala65, the monodentate Asp59, Asn61 and Asp63, the bidentate Glu70 and a water molecule) interact with calcium, forming a pentagonal bipyramidal coordination. The case of seven oxygen ligands binding calcium ion has been reported in other S100 proteins, namely holo psoriasin, holo calbindin and troponin-C (Herzberg & James, 1985; Szebenyi & Moffat, 1986; Brodersen *et al.*, 1998).

The main-chain structures of EF-1 and EF-2 in the two MRP8 monomers are compared with holo calbindin (Szebenyi & Moffat, 1986) and holo S100B (Smith & Shaw, 1998) in Fig. 4. The EF-1 of MRP8 is similar to that of calbindin and S100B except for the N-terminus, but EF-2 is somewhat different. Helix IV of MRP8 is longer than the corresponding helix in calbindin by one turn. It is likely that the interhelix angle of helix I–II is similar (Table 3), but it is more divergent in helix III–IV. Moreover, helix IV of the two MRP8 monomers is somewhat different at the C-terminus (r.m.s. deviation is 0.51 Å). Thus, the C-terminal helix (helix IV) is more variable in shape. It has been proposed that helix IV may be important in cases where many similar calcium-binding proteins distinguish their cognate target molecules from other proteins (Hilt & Kligman, 1991).

3.3. Difference of two EF-hands

In the Ca^{2+}-bound crystal of MRP8, the electron density corresponding to the Ca^{2+} ion in EF-2 was higher than that in EF-1. This difference was confirmed by the temperature factors of these atoms after structure refinement. The *B* factors of Ca^{2+} in EF-1 are 33.06 and 35.63 $Å^2$ for the two independent monomers, while they are 11.29 and 13.41 $Å^2$ in EF-2. (The occupancies of both sites were kept at unity throughout the refinements.) This is consistent with the previous observation that EF-2 has a higher affinity than EF-1 for Ca^{2+} (Kligman & Hilt, 1988; Rammes *et al.*, 1997). In this context, it may be of interest to note the molecular behaviour observed during the course of preparing a heavy-atom derivative. For structure analysis by the MAD method, we attempted to replace the calcium ion with a ytterbium ion prior to crystallization. In the ytterbium-substituted crystal, the calcium ion in EF-2 was replaced by a ytterbium ion, whereas the calcium ion in EF-1 remained bound as judged from the initial electron-density map and the anomalous difference Fourier map of the ytterbium-substituted crystal; the latter map showed no peak at the ion-binding site. This view was confirmed by the temperature factors of the atoms assigned as calcium (33.2 and 34.8 $Å^2$ for the two independent monomers) after the structure refinement. Thus, while EF-2 has a higher affinity for calcium ions than EF-1, it can also more easily release the calcium ions upon environmental change. These are clearly favourable characteristics for the calcium switch. This feature can be rationally explained by the difference in calcium ligands between the two sites; the calcium ligand of EF-2 is mostly side chains, compared with the main-chain carbonyl O atom in EF-1. EF-2 may not need to pass though an energetically unfavourable transition state during the course of ion exchange.

A relevant observation was the case of holmium-bound psoriasin, where the calcium ion in the C-terminal EF-hand was substituted by a holmium ion and the N-terminal EF-hand has no bound atom. However, in this case the N-terminal EF-hand has three residues deleted (Fig. 2) and may have no calcium-binding capacity (Brodersen *et al.*, 1998). In the case of the half-saturated cadmium state of calbindin, EF-2 was occupied by a cadmium ion but EF-1 was unoccupied (Akke *et al.*, 1995). In the latter case, the structure exhibited a large difference before and after cadmium binding. This structure is more similar to that of the fully calcium-saturated state.

The calcium-triggered conformational change is the first step in the binding of the S100 family of proteins to their cognate target molecules. It has previously been shown that S100B, one of the S100 family of proteins, undergoes a large conformational change upon calcium binding (Smith & Shaw, 1998; Matsumura *et al.*, 1998). The backbone reorientation of the N-terminus of EF-2 leads to a change in the position of helix III relative to other helices close to the molecular centre (helices I and IV), resulting in the exposure of the hydrophobic residues at helix IV. Based on these observations, it was proposed that the S100 molecule binds target molecules by the

exposed hydrophobic residues in a similar way to calmodulin (Matsumura *et al.*, 1998).

The xenon-binding site we found provides further support for this idea. During the course of the heavy-atom search, we prepared a MRP8–xenon complex by diffusion of xenon gas into the MRP8 crystal at high pressure (0.7 and 2 MPa) using a device similar to that developed by Stowell *et al.* (1996). The difference Fourier map at 2.0 Å revealed that three Xe atoms

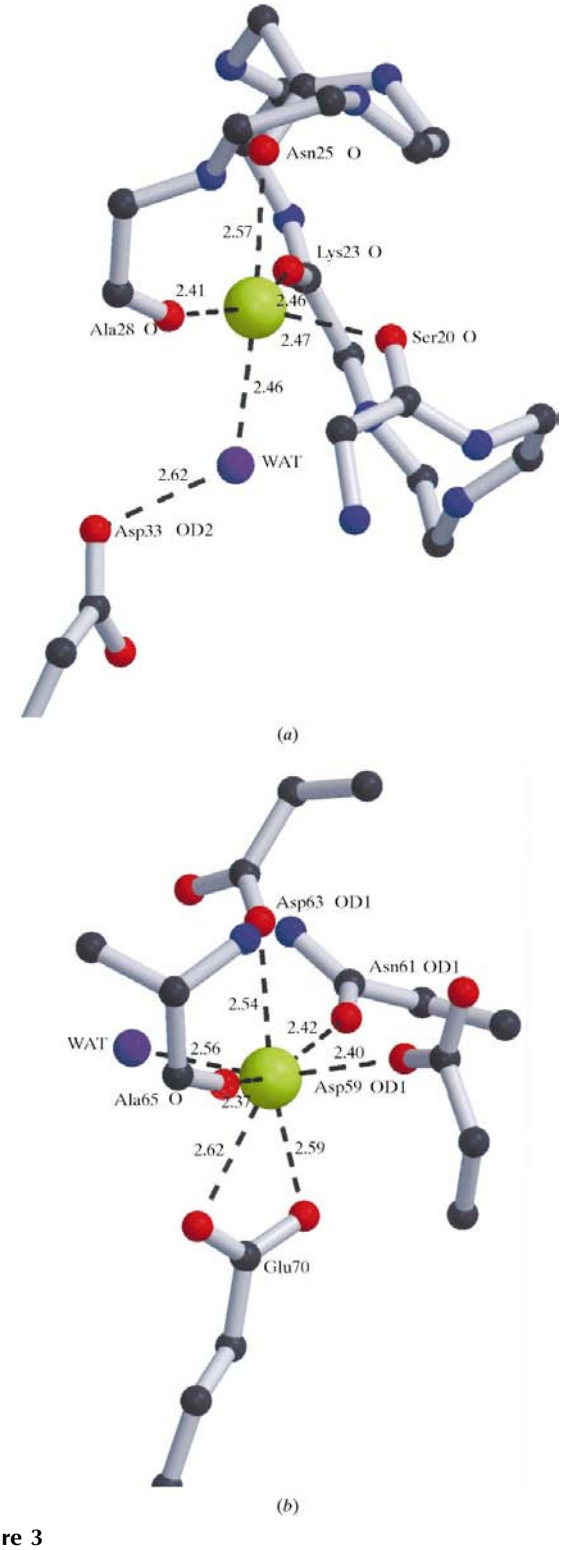

Figure 3
Tube representation of the EF-hands in MRP8. (*a*), EF-1; (*b*), EF-2. Calcium ions are shown as yellow spheres, O atoms in red, N atoms in blue, C atoms in black and water molecules in purple.

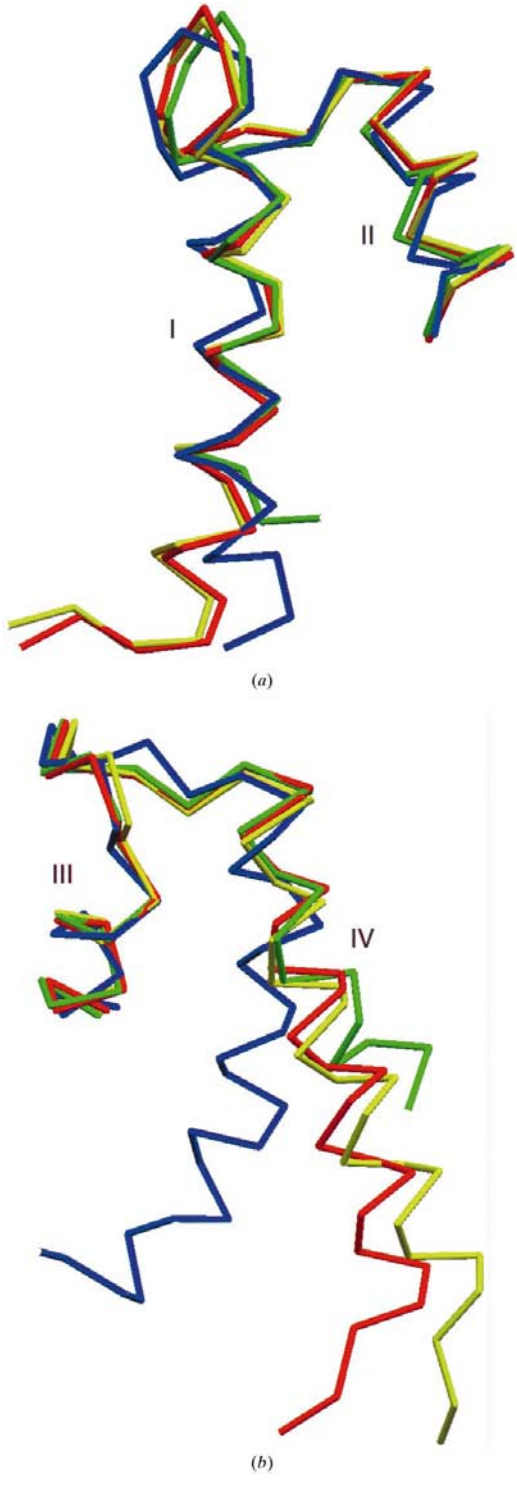

Figure 4
The main-chain superposition of the EF-hands. (*a*) EF-1, (*b*) EF-2. Human MRP8 (residues Met1–Glu41) is shown in red (chain *A*) and yellow (chain *B*), human holo S100B (Ser1–Glu39) in blue and bovine holo calbindin (Lys1–Glu35) in green. The viewed residues are Gly51–Ser90 for MRP8; Val53–Glu90 for S100B and Leu46–Gln75 for calbindin.

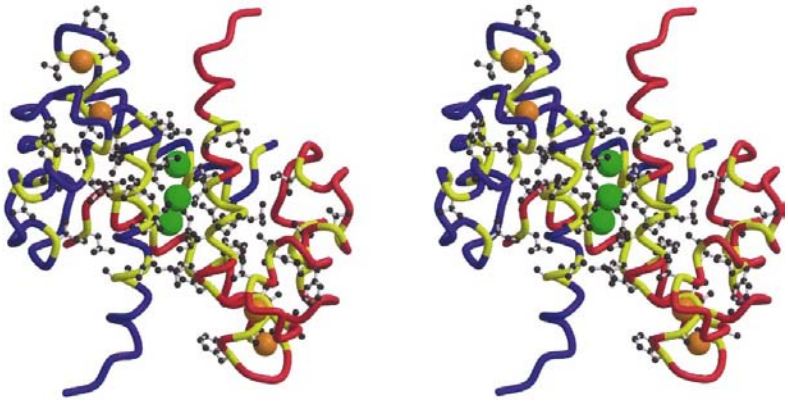

Figure 5
Stereo drawing of MRP8 dimer showing trapped Xe atoms in a hydrophobic cavity created at the monomer interface. Xe atoms are shown as green spheres. The main chains of the two independent monomers are shown in different colours (blue and red), with their hydrophobic parts in yellow. Hydrophobic side chains are also shown. Ca atoms are shown in orange.

were located in a row in a cavity created at the dimer interface (Fig. 5) where the hydrophobic residues Val, Leu, Ile and Phe were clustered. The distances between each Xe atom and the neighbouring atoms were in the range 2.9–4.8 Å. It is well known that Xe atoms are trapped in the hydrophobic cavity. Although no complex structure between S100 and target molecules has been analyzed so far, the xenon-complex structure demonstrates that the cavity created between two α-helices (helices IV and IV′) works as a binding site for the hydrophobic molecules.

4. Conclusions

MRP8 and MRP14 are members of the S100 family, the largest subfamily of EF-hand proteins that are involved in calcium-dependent enzyme activation, regulation of cellular differentiation and cell-cycle progression (Kligman & Hilt, 1988; Persechini *et al.*, 1989; Schäfer & Heizmann, 1996). Although no definite function could be assigned to these two proteins, their expressions are largely confined to myeloid cell lineage: granulocytes, monocytes and macrophages (Odink *et al.*, 1987; Lagasse & Clerc, 1988). Recently, it was reported that MRP8 and MRP14 possess the potential to bind arachidonic acid depending on the intracellular Ca^{2+} level, showing that elevation of Ca^{2+} might stimulate the translocation of these from the cytoplasm to the plasma membrane as well as to intermediate filaments (Klempt *et al.*, 1997). In this context, a molecular-basis study on the biological activities of these proteins with Ca^{2+} appears to be important.

In this study, we have demonstrated the three-dimensional structure of MRP8 in complexes formed with Ca^{2+} and Yb^{3+}. The structure of the Ca^{2+}-bound form showed that EF-2 binds Ca^{2+} more tightly than EF-1. This is consistent with previous reports that the C-terminal EF-hands of other S100 family proteins exhibit a significantly higher affinity for Ca^{2+} than do the N-terminal EF-hand domains, and that the N-terminal EF-hand can bind Ca^{2+} only at higher concentrations (Kligman & Hilt, 1988; Rammes *et al.*, 1997). However, an unexpected result was obtained when calcium was replaced with ytterbium. The structure of the Yb^{3+}-substituted form of MRP8 showed that only the calcium ion in the EF-2 site was actually replaced by Yb^{3+}. Furthermore, it was demonstrated that Xe atoms can be accommodated in the hydrophobic cavity created between two α-helices. It is thus conceivable that the structural change of S100 protein induced by Ca^{2+} observed in previous experiments (Zwadlo *et al.*, 1988; Matsumura *et al.*, 1998) may be triggered by the binding of Ca^{2+} to the C-terminal EF-hand (EF-2) site.

The present results are also consistent with the finding that MRP8 and MRP14 exert biological activities in a Ca^{2+} concentration dependent manner. Some modification of the EF-hand structure by means of site-directed mutagenesis, with regard to Ca^{2+}-binding capacity, will lead to further insight into evaluation of the molecular function of MRP8 as well as MRP14. Experiments on this are currently under way.

We thank N. Sakabe, N. Watanabe, M. Suzuki and N. Igarashi of the Photon Factory, National Laboratory for High Energy Physics, Japan, and H. Sugimoto of Hokkaido University for their kind help in data collection. We also thank E. Muto for her kind assistance with protein purification and crystallization. This work was partly supported by the 'Research for the Future' Program (JSPS-RFTF 97 L00501) from the Japan Society for the Promotion of Science.

References

Abrahams, J. P. & Leslie, A. G. W. (1996). *Acta Cryst.* D**52**, 30–42.
Akke, M., Forsén, S. & Chazin, W. J. (1995). *J. Mol. Biol.* **252**, 102–121.
Brodersen, D. E., Etzerodt, M., Madsen, P., Celis, J. E., Thogersen, H. C., Nyborg, J. & Kjeldgaard, M. (1998). *Structure*, **6**, 477–489.
Brünger, A. T. (1992). *Nature (London)*, **355**, 472–475.
Brünger, A. T. (1993). *X-PLOR Version* 3.1. *A System for X-ray Crystallography and NMR*. New Haven, CT, USA: Yale University Press.
Brünger, A. T., Krukowski, A. & Erickson, J. (1990). *Acta Cryst.* A**46**, 585–593.
Brünger, A. T., Kuriyan, J. & Karplus, M. (1987). *Science*, **235**, 458–460.
Burmeister, G., Tarcsay, L. & Sorg, C. (1986). *Immunobiology*, **171**, 461–474.
Collaborative Computational Project, Number 4 (1994). *Acta Cryst.* D**50**, 760–763.
Delabie, J., de Wolf-Peeters, C., van den Oord, J. J. & Desmet, V. J. (1990). *Clin. Exp. Immunol.* **81**, 123–126.
Fortelle, E. de la & Bricogne, G. (1997). *Methods Enzymol.* **276**, 472–494.
Hendrickson, W. A. (1991). *Science*, **254**, 51–58.
Herzberg, O. & James, M. N. (1985). *Nature (London)*, **313**, 653–659.

Hilt, D. C. & Kligman, D. (1991). *The S-100 Protein Family: a Biochemical and Functional Overview. Novel Calcium-Binding Proteins*, edited by C. W. Heizmann, pp. 65–103. New York: Springer–Verlag.
Jiang, J. S. & Brünger, A. T. (1994). *J. Mol. Biol.* **243**, 100–115.
Jones, T. A., Zou, J. Y., Cowan, S. W. & Kjeldgaard, M. (1991). *Acta Cryst.* A**47**, 110–119.
Klempt, M., Melkonyan, H., Nacken, W., Wiesmann, D., Holtkemper, U. & Sorg, C. (1997). *FEBS Lett.* **408**, 81–84.
Kligman, D. & Hilt, D. C. (1988). *Trends Biochem. Sci.* **13**, 437–443.
Kraulis, P. J. (1991). *J. Appl. Cryst.* **24**, 946–950.
Lagasse, E. & Clerc, R. G. (1988). *Mol. Cell. Biol.* **8**, 2402–2410.
Lamzin, V. S. & Wilson, K. S. (1993). *Acta Cryst.* D**49**, 129–147.
Laskowski, R. A., MacArthur, M. W., Moss, D. S. & Thornton, J. M. (1993). *J. Appl. Cryst.* **26**, 283–291.
McPherson, A. Jr (1976). *Methods Biochem. Anal.* **23**, 249–345.
Matsumura, H., Shiba, T., Inoue, T., Harada, S. & Kai, Y. (1998). *Structure*, **6**, 233–241.
Merrit, E. A. & Murphy, M. E. P. (1994). *Acta Cryst.* D**50**, 869–873.
Miyahara, J., Takahashi, K., Amemiya, Y., Kamiya, N. & Satow, Y. (1986). *Nucl. Instrum. Methods A*, **246**, 572–578.
Odink, K., Cerletti, N., Brüggen, J., Clerc, R. G., Tarcsay, L., Zwadlo, G., Gerhards, G., Schlegel, R. & Sorg, C. (1987). *Nature (London)*, **330**, 80–82.
Otwinowski, Z. (1993). *Proceedings of the CCP4 Study Weekend: Data Collection and Processing*, edited by L. Sawyer, N. Isaacs & S. Bailey, pp. 56–62, Warrington: Daresbury Laboratory.
Persechini, A., Moncrief, N. D. & Kretsinger, R. H. (1989). *Trends Neurosci.* **12**, 462–467.
Rammes, A., Roth, J., Goebeler, M., Klempt, M., Hartmann, M. & Sorg, C. (1997). *J. Biol. Chem.* **272**, 9496–9502.
Sakabe, N., Ikemizu, S., Sakabe, K., Higashi, T., Nakagawa, A., Watanabe, N., Adachi, S. & Sasaki, K. (1995). *Rev. Sci. Instrum.* **66**, 1276–1281.
Sastry, M., Ketchem, R. R., Crescenzi, O., Weber, C., Lubienski, M. J., Hidaka, H. & Chazin, W. J. (1998). *Structure*, **6**, 223–231.
Schäfer, B. W. & Heizmann, C. W. (1996). *Trends Biochem. Sci.* **21**, 134–140.
Smith, S. P. & Shaw, G. S. (1998). *Structure*, **6**, 211–222.
Stowell, M. H. B., Soltis, S. M., Kisker, C., Peters, J. W., Schindelin, H., Rees, D. C., Cascio, D., Beamer, L., Hart, P. J., Wiener, M. C. & Whitby, F. G. (1996). *J. Appl. Cryst.* **29**, 608–613.
Szebenyi, D. M. & Moffat, K. (1986). *J. Biol. Chem.* **261**, 8761–8777.
Teigelkamp, S., Bhardwaj, R. S., Roth, J., Meinardus-Hager, G., Karas, M. & Sorg, C. (1991). *J. Biol. Chem.* **266**, 13462–13467.
Zwadlo, G., Brüggen, J., Gerhards, G., Schlegel, R. & Sorg, C. (1988). *Clin. Exp. Immunol.* **72**, 510–515.